Future Foods 14 (2026) 101109

Contents lists available at ScienceDirect

Future Foods

journal homepage: www.elsevier.com/locate/fufo

Rice-shaped soy protein isolate–alginate–carrageenan hydrogel: Physicochemical properties and digestion-associated release behavior

Mutthatinee Tangmongkhonsuk [a], Siriyakorn Chantieng [a], Vernabelle Balmori [b], Kasinee Katelakha [c], Nureesun Mahamud [c], Charoonsri Chusak [a], Nazimah Hamid [d], Sirichai Adisakwattana [a,*]

[a] Center of Excellence in Phytochemical and Functional Food for Clinical Nutrition, Department of Nutrition and Dietetics, Faculty of Allied Health Sciences, Chulalongkorn University, Bangkok, 10330, Thailand
[b] Department of Food Science and Technology, Southern Leyte State University, Southern Leyte, Sogod, 6606, Philippines
[c] The Halal Science Center, Chulalongkorn University, Bangkok, 10330, Thailand
[d] Centre for Future Foods, Auckland University of Technology, Auckland, New Zealand

ARTICLE INFO

Keywords:
Soy protein isolate
Encapsulation
Carrageenan
Digestion-associated release
Rice-shaped hydrogel

ABSTRACT

White rice is widely consumed as a staple food in many Asian populations, although it generally provides limited amounts of dietary fiber, micronutrients, and phytochemicals. Rice-shaped hydrogel systems may offer a potential structuring approach for incorporating plant-based protein ingredients into visually familiar food format. This study investigated the feasibility of forming rice-shaped soy protein isolate (SPI)–alginate–carrageenan hydrogel containing 4–8% SPI in alginate matrices (1.8%, w/v), with or without carrageenan (0–1%, w/v). Physicochemical, structural, and digestion-associated release properties were evaluated, and principal component analysis was used as a supportive tool to summarize formulation-dependent differences. Increasing SPI concentration influenced yield, water absorption, encapsulation efficiency, and textural properties. Carrageenan-containing formulations showed differences in morphology, hydration behavior, and SPI retention, suggesting possible changes in matrix organization. FTIR and XRD analyses indicated structural differences among formulations, potentially associated with interactions among SPI, alginate, carrageenan, and calcium ions. During simulated digestion, the ninhydrin assay indicated formulation-dependent release of amino-group-containing residues, with SPI8C1 showing the highest response, although this may partly reflect its higher initial SPI loading. Targeted LC–MS analysis detected selected isoflavone-associated compounds, including genistin, daidzin, and genistein, in SPI-containing hydrogel formulations. Overall, this study provides proof-of-concept information on formulation-dependent physicochemical, structural, and digestion-associated release properties of rice-shaped SPI–alginate–carrageenan hydrogels. Among the tested formulations, SPI8C1 exhibited the highest encapsulation efficiency and amino-group-containing residue release response, while carrageenan incorporation influenced hydration behavior, morphology, and matrix organization.

1. Introduction

Rice is a staple food for billions of people worldwide, particularly in Asia, where it provides the primary source of dietary energy (Lai et al., 2023). However, polished white rice generally provides limited amounts of dietary fiber, minerals, and phytochemicals. Polished rice typically contains approximately 6–8% protein on a dry weight basis and is limited in lysine, the first limiting amino acid in cereals, resulting in moderate protein quality. These nutritional characteristics have encouraged interest in exploring rice-shaped structured matrices for incorporating complementary plant-based protein ingredients.

Soy protein isolate (SPI) contains more than 90% protein and has a protein digestibility-corrected amino acid score (PDCAAS) of 1.0, indicating high protein density and amino acid completeness compared with cereal-based protein sources (Hertzler et al., 2020). SPI may also contain isoflavone-associated compounds, including genistein and daidzin derivatives, which have been associated with antioxidant and other health-related properties (Barańska et al., 2021). SPI has been widely

* Corresponding author.
E-mail address: Sirichai.a@chula.ac.th (S. Adisakwattana).

https://doi.org/10.1016/j.fufo.2026.101109
Received 15 December 2025; Received in revised form 2 June 2026; Accepted 25 June 2026
Available online 25 June 2026

incorporated into food products such as protein beverages, bakery products, and meat analogs (Huang et al., 2024). Nevertheless, sensory characteristics associated with soy proteins may influence consumer perception in some food applications (Vatansever et al., 2024). Therefore, alternative structuring strategies may provide opportunities for developing alternative plant-protein-enriched food systems.

Hydrogel-based structuring may provide a potential approach for incorporating proteins and selected bioactive-associated compounds into food matrices. Alginate-based hydrogels are widely used in food applications because of their non-toxicity, biocompatibility, and gel-forming ability in the presence of calcium ions. Carrageenan can be used as a co-hydrocolloid to modify alginate-based matrices, potentially influencing texture, hydration behavior, encapsulation efficiency, and matrix organization (Postolović et al., 2022). The combination of alginate and carrageenan may therefore provide a useful model system for studying SPI incorporation into rice-shaped hydrogel matrices. In the present study, the hydrogel system was investigated as a structuring approach for incorporating SPI into rice-shaped formulations.

Recent studies on rice analogs and fortified rice products have explored the incorporation of proteins, fibers, and other functional ingredients into rice-like formats. However, many systems rely on starch-based matrices or extrusion-based processing, which may influence texture, cooking stability, and ingredient retention during processing and digestion (Chaturvedi and Manickavasagan, 2024). In this context, hydrogel structuring offers an alternative method for forming rice-shaped particles and evaluating formulation-dependent physicochemical and digestion-associated release properties.

The rice-shaped format in the present study was selected to provide a visually familiar morphology for rice-consuming populations. Because the formulation does not contain rice flour or rice starch, the developed samples were designed as rice-shaped SPI–alginate–carrageenan hydrogels rather than conventional rice analog products. In light of these considerations, the present study aimed to investigate the feasibility of forming rice-shaped SPI–alginate–carrageenan hydrogel systems using alginate as the primary matrix and carrageenan as a co-structuring hydrocolloid. Furthermore, the study also aimed to evaluate formulation-dependent physicochemical properties, structural characteristics, antioxidant-related responses, and digestion-associated release behavior under a simplified simulated gastrointestinal model. Principal component analysis was used as a supportive tool to summarize relationships among formulation variables and measured properties. The findings provide proof-of-concept information on the structuring and digestion-associated release characteristics of SPI-containing hydrogel matrices.

2. Materials and methods

2.1. Materials

Sodium alginate, κ-carrageenan, calcium chloride, and food-grade soy protein isolate (SPI) powder were purchased from Krungthepchemi Co., Ltd. (Bangkok, Thailand). Folin–Ciocalteu's reagent, porcine pepsin (250 U/mg), α-amylase Type VI-B from porcine pancreas (15.8 U/mg), pancreatin (4 × USP), amyloglucosidase (3,260 U/mL), 2,2-diphenyl-1-picrylhydrazyl (DPPH), and gallic acid were obtained from Sigma-Aldrich, Inc. (St. Louis, MO, USA).

2.2. Preparation of SPI rice-shaped grains

SPI rice-shaped grains were prepared following a modified ionic gelation encapsulation method, adapted from Chantieng et al. (2025). Sodium alginate (1.8% w/v) was dissolved in distilled water (500 mL) at 60 °C under continuous magnetic stirring (600 rpm) until a clear homogeneous solution was obtained. SPI powders were dispersed in distilled water to obtain final concentrations of 4, 6, and 8% (w/v), and the solutions were mixed with the alginate solution at a ratio of 1:1 (v/v). Carrageenan (0.5–1% w/v) was added to selected formulations and dissolved under mild heating (50 °C) until complete hydration, while control formulations were prepared without carrageenan. The mixed solutions were allowed to stand at room temperature (25 °C) for 1 h to ensure full hydration and polymer network formation.

The final mixtures were transferred into sterile plastic piping bags and extruded dropwise into a gently stirred calcium chloride solution (1.5% w/v, 500 mL) using a consistent drop size (2–3 mm diameter). Rice-shaped grains were formed by cutting the extruded droplets with a sterile blade at ~1 cm interval, producing cylindrical particles resembling polished rice. The grains were allowed to harden in the $CaCl_2$ bath for 3 min under static conditions to enable ionic cross-linking of alginate chains.

Calcium chloride (E509) is an approved food-grade additive widely used in food processing applications such as tofu production, fruit firming, and vegetable stabilization, and has been evaluated as safe by regulatory authorities (EFSA 2012). Calcium-mediated alginate gelation is a well-established and widely accepted technique in food systems (Lee & Mooney, 2012). Therefore, the residual calcium level in the final product is expected to be low and within the range typical of alginate-based food applications, without posing biosafety concerns. The calcium incorporated through cross-linking is structurally bound within the hydrogel matrix and is unlikely to significantly contribute to total dietary calcium intake. The calcium content of the final product was further determined by ALS Laboratory Group (Thailand) Co., Ltd. using an in-house method (STM No.05-013) based on AOAC (2023) Official Method 984.27, and was found to be approximately 205 mg per 100 g. This level corresponds to about 20.5% of the recommended dietary allowance (RDA) for adults (1,000 mg/day) and remains well below the tolerable upper intake level (2,000–2,500 mg/day), indicating that the product is safe for consumption under normal dietary conditions (National Academies of Sciences, Engineering, and Medicine, 2011). The grains were then drained on filter paper and stored in airtight polyethylene containers at 4 °C for up to 48 h prior to analysis to prevent structural dehydration.

2.3. Water Absorption (WA) of SPI-based rice-shaped grains

Water absorption was determined following the AACC method (AACC, 1988) with slight modifications. SPI rice-shaped grain samples were boiled in distilled water (100 °C) at a sample-to-water ratio of 1:10 (w/v) for 1 min. After boiling, the samples were drained, and excess surface moisture was gently removed prior to weighing. WA was calculated as:

$$\text{Water absorption } (\%) = \frac{\text{Weight of cooked SPI rice} - \text{Weight of uncooked SPI rice}}{\text{Weight of raw SPI rice}} \times 100$$

2.4. Texture Profile Analysis (TPA)

The texture of cooked SPI rice-shaped grains was measured using a Texture Analyzer TA.XT2i (Stable Micro Systems, Surrey, UK) equipped with a cylindrical probe (P/50). Each sample was compressed twice to 75% of its original height at pre-test, test, and post-test speeds of 1 mm/s. Textural parameters including hardness, springiness, cohesiveness, gumminess, adhesiveness, and chewiness were calculated from the force–time curves.

2.5. Encapsulation Efficiency (%EE)

Encapsulation efficiency (%EE) was determined using the ninhydrin colorimetric assay adapted from Chusak et al. (2020). In this assay, free amino groups released from amino acids, peptides, and other amino-group-containing compounds react with ninhydrin reagent to form a purple chromophore, the intensity of which reflects amino-group-containing equivalents. SPI rice-shaped grain samples were dissolved in sodium citrate solution (5% w/v) to disrupt the alginate matrix, followed by centrifugation at 10,000 rpm for 15 min to obtain the supernatant Chantieng et al. (2025).The concentration of amino-group-containing equivalents in the supernatant was quantified using the ninhydrin assay and expressed as lysine equivalents based on a lysine calibration standard (1.56–200 μg/mL). Absorbance was measured at 568 nm using a microplate reader (PowerWave XS2, BioTek, USA). Encapsulation efficiency was calculated as:

$$\text{Encapsulation efficiency (\%EE)} = \frac{P_r}{P_t} \times 100$$

Where P_t represents the total amount of SPI-derived amino-group-containing equivalents initially added to the SPI rice-shaped grain formulation, and P_r represents the amount of SPI-derived amino-group-containing equivalents recovered from the SPI rice-shaped grains after disruption of the hydrogel matrix.

2.6. Quality properties of SPI-based rice-shaped grains

The yield of SPI rice-shaped grains was determined according to a modified method of Xie et al. (2025). The weight of the SPI–alginate mixture was recorded prior to extrusion into the $CaCl_2$ solution (1.5% w/v). Following gelation, the rice-shaped products were rinsed with distilled water, drained, and weighed to obtain the final product weight. Product yield (%) was calculated as:

$$\text{Yield (\%)} = \frac{W_f}{W_i} \times 100$$

where Wf represents the weight of the final SPI rice-shaped grains after gelation, rinsing, and draining, and Wi represents the weight of the initial SPI–alginate mixture before extrusion.

2.7. Color measurement

Color parameters (L^*, a^*, b^*) of the cooked SPI rice-shaped grains were measured using a colorimeter (Hunter Lab Color Flex EZ 45/0°, Hunter Lab Inc., Virginia, USA). The instrument was calibrated using a standard white reference plate prior to measurement. Three independent measurements were recorded for each sample, and mean values were reported.

2.8. Determination of phytochemical compounds by targeted LC–MS

Targeted LC–MS/MS analysis was performed for the preliminary characterization of selected isoflavone-associated compounds in rice-shaped SPI–alginate–carrageenan hydrogel samples, following a modified method of Peanparkdee et al. (2019). Briefly, 10 g of sample was pulverized, homogenized with 20 mL of 0.1% formic acid in methanol, stirred for 30 min, and filtered through a 0.22 μm nylon syringe filter. The filtrate was centrifuged at 12,000 rpm for 10 min at 25 °C, and the supernatant was desiccated at 40 °C for 24 h. The dried extract was reconstituted in 100 μL of 0.1% formic acid in methanol, centrifuged, and transferred to glass vials for analysis.

LC–MS/MS analysis was performed using a Dionex Ultimate 3000 UHPLC system coupled with a QTOF Impact II mass spectrometer (Bruker Daltonics, Bremen, Germany). Separation was achieved on a Hypersil GOLD C18 column (2.1 × 100 mm, 1.9 μm) at 40 °C, with solvent A consisting of 0.1% formic acid in water and solvent B consisting of acetonitrile. The gradient elution was as follows: 0–15 min, 0–99% B; 15–20 min, held at 99% B; and 20.1–25 min, 1% B. The flow rate was 0.3 mL/min, and the injection volume was 3 μL. Electrospray ionization was operated in positive mode with a mass range of m/z 50–1200, drying gas temperature of 250 °C, and capillary voltage of 3800 V.

Isoflavones, including genistin, genistein, and daidzin, were identified based on retention time, m/z values, and mass spectral information compared with authentic standards. Quantification was performed using external calibration curves prepared from authentic standards over the concentration range of 0–0.01 mg/mL using four concentration points. The calibration curve coefficients (R^2) were 0.9955 for genistin, 0.9795 for daidzin, and 0.9801 for genistein. Representative chromatographic profiles of authentic standards are provided in Supplementary Fig. S1. This analysis focused on selected isoflavone-associated compounds in SPI-containing hydrogel formulations using a targeted LC–MS/MS approach.

2.9. Fourier Transform Infrared Spectroscopy (FTIR) analysis

The structural interactions among SPI, alginate, and carrageenan in SPI rice-shaped grains were analyzed using FTIR spectroscopy (Alpha II, Bruker, Massachusetts, USA). Spectra were recorded from 675–4000 cm^{-1} with four scans per sample. Cooked SPI rice-shaped grain samples were semi-dried at 25 °C for 6 h, and ~2 mg of each sample was placed on the sample holder. Characteristic absorption bands were evaluated to identify formulation-dependent structural features among the hydrogel samples.

2.10. X-ray Diffraction (XRD) analysis

The crystalline structure of SPI rice-shaped grains was examined using an X-ray diffractometer (Bruker AXS D8 Discover, Leipzig, Germany) equipped with a copper tube (40 kV, 45 mA). Diffraction patterns were collected over a 2θ range of 5–40° at a scanning rate of 0.02° 2θ/s. Cooked SPI rice-shaped grain samples were semi-dried at 25 °C for 6 h, and ~1 g of sample was analyzed. Relative crystallinity (%) was calculated from the ratio of crystalline to total diffraction areas.

$$\text{\% Relative crystallinity} = \frac{\text{Area above the smooth curve}}{\text{Total diffraction area above the baseline}} \times 100$$

2.11. Digestion-associated release analysis under a simplified simulated gastrointestinal model

Digestion-associated release analysis was performed following the method of Suklaew et al. (2020) with slight modifications. The assay was conducted to evaluate digestion-associated release behavior under simplified simulated gastrointestinal conditions. Digestion was conducted in three sequential phases: oral, gastric, and small intestinal. For the oral phase, two grams of rice-shaped SPI–alginate–carrageenan hydrogel samples were mixed with 1 mL of artificial saliva containing amylase (10 U/mL in 0.2 M carbonate buffer). Gastric phase digestion was initiated by adding the sample to 5 mL of porcine pepsin solution (1

mg/mL in 0.02 M HCl), adjusting the pH to 2.0 ± 0.1, and incubating at 37 °C in a covered shaking water bath for 30 min. After digestion, the pH was adjusted to 4.5 by adding 5 mL of 0.02 M NaOH and 25 mL of 0.2 M sodium acetate buffer to inactivate pepsin. The gastric digesta was collected, and enzymatic activity was terminated by heating at 100 °C for 10 min, followed by centrifugation (10,000 rpm, 15 min, 4 °C). Supernatants were stored at −20 °C until analysis. For the small intestinal phase, digestion was carried out by adding an enzyme solution containing 5 mL of pancreatin (2 mg/mL), amyloglucosidase (28 U/mL), and bile acid (10 mg/mL) in 0.2 M sodium acetate buffer. Aliquots of digesta were collected at 0, 20, 30, 60, 90, 120, and 180 min. Enzymatic reactions were terminated by heating at 100 °C for 10 min, and samples were centrifuged (10,000 rpm, 15 min, 4 °C). The supernatants were stored at −20 °C for further analysis.

2.12. Release of amino-group-containing residues using the ninhydrin colorimetric assay

The release of amino-group-containing residues from digested rice-shaped SPI–alginate–carrageenan hydrogel samples was assessed using the ninhydrin colorimetric assay, following the procedure described in Section 2.5. The ninhydrin assay detects free amino groups derived from amino acids, peptides, and other amino-group-containing compounds present in the digested supernatant.

2.13. Total Phenolic Content (TPC)

The release of phenolic-associated compounds from digested rice-shaped SPI–alginate–carrageenan hydrogel samples was quantified using the Folin–Ciocalteu method (Wongverawattanakul et al., 2022). Briefly, 50 µL of digested supernatant was mixed with 50 µL of 10% (v/v) Folin–Ciocalteu reagent and incubated at room temperature for 5 min. Then, 50 µL of sodium carbonate solution (20% w/v) was added, and the mixture was kept in the dark for 30 min. Absorbance was measured at 760 nm, and results were expressed as mg gallic acid equivalents (GAE) per mL of digesta (mg GAE/mL). Because the Folin–Ciocalteu assay is a chemical colorimetric method, the results were interpreted as phenolic-associated reducing capacity under the applied experimental conditions.

2.14. Antioxidant-Related Responses (FRAP Assay)

Antioxidant-related responses of digested rice-shaped SPI–alginate–carrageenan hydrogel samples were assessed using the ferric reducing antioxidant power (FRAP) assay according to Ren et al. (2018). The FRAP reagent was prepared by mixing 10 mM 2,4,6-tris(2-pyridyl)-s-triazine (TPTZ) in 40 mM HCl, 20 mM $FeCl_3$, and acetate buffer (pH 3.6) at a ratio of 1:1:10 (v/v/v), followed by incubation for 1 h at 37 °C. A 5 µL aliquot of digested supernatant was mixed with 150 µL of FRAP reagent and incubated at 37 °C for 30 min. Absorbance was measured at 593 nm using a spectrophotometer, with distilled water as the blank. Results were calculated from a a Trolox standard curve and expressed as µmol Trolox equivalents per mL of digesta (µmol TE/mL).

2.15. Statistical analysis

All experiments were performed in triplicate, and results were expressed as mean ± standard error of the mean (SEM, n = 3). Differences among means were assessed using one-way analysis of variance (ANOVA) followed by Tukey's post hoc test, with statistical significance set at $p < 0.05$. Statistical analyses were conducted using SPSS software (version 29.0; IBM Corp., Armonk, NY, USA).

Principal component analysis (PCA) was conducted in R (version 4.2.3; R Core Team, 2020) using the FactoMineR package. Data were normalized prior to analysis, and Pearson's correlation matrix was applied to explore the relationships among variables. Components were retained based on eigenvalues greater than 1 and cumulative variance explained, and loading plots were used to visualize the contribution of physicochemical, textural, and encapsulation parameters to sample separation.

Table 1
Physicochemical, color, and texture properties of SPI-based rice-shaped formulations.

Parameters	SPI4	SPI6	SPI8	SPI4C0.5	SPI6C0.5	SPI8C0.5	SPI4C1	SPI6C1	SPI8C1
Yield (%)	63.76 ± 1.68^{c}	70.73 ± 3.62^{ab}	71.12 ± 1.87^{ab}	64.15 ± 0.12^{c}	71.14 ± 0.25^{ab}	73.39 ± 0.29^{a}	66.47 ± 1.10^{bc}	71.59 ± 1.44^{ab}	75.82 ± 2.83^{a}
Water absorption (%)	16.41 ± 2.48^{d}	25.26 ± 2.56^{ab}	26.32 ± 3.67^{ab}	18.90 ± 1.39^{cd}	25.63 ± 0.05^{ab}	27.89 ± 0.23^{ab}	23.34 ± 4.75^{b}	26.09 ± 2.37^{ab}	29.60 ± 1.37^{a}
Encapsulation efficiency (%)	50.86 ± 0.56^{f}	55.65 ± 0.12^{de}	60.67 ± 0.22^{d}	52.75 ± 0.12^{ef}	58.33 ± 0.55^{cd}	70.86 ± 0.05^{b}	58.26 ± 1.34^{d}	65.85 ± 0.46^{c}	81.08 ± 1.53^{a}
Lightness (L^*)	41.61 ± 0.23^{a}	41.42 ± 0.08^{ab}	40.91 ± 0.07^{c}	41.40 ± 0.15^{ab}	41.31 ± 0.03^{ab}	40.40 ± 0.16^{d}	41.29 ± 0.15^{ab}	41.18 ± 0.04^{bc}	39.61 ± 0.12^{e}
Redness (a^*)	0.047 ± 0.01^{c}	0.37 ± 0.16^{b}	1.07 ± 0.11^{a}	0.047 ± 0.05^{c}	0.25 ± 0.09^{bc}	0.98 ± 0.84^{a}	0.04 ± 0.01^{c}	0.18 ± 0.01^{bc}	0.85 ± 0.16^{a}
Yellowness (b^*)	12.42 ± 0.12^{e}	14.47 ± 0.36^{bc}	15.35 ± 0.15^{a}	11.58 ± 0.24^{f}	14.04 ± 0.42^{c}	15.04 ± 0.66^{ab}	11.48 ± 0.15^{f}	13.12 ± 0.03^{d}	14.88 ± 0.16^{ab}
Texture profile									
Hardness (g)	11,464.59 ± 21.73^{a}	9,951.08 ± 24.97^{b}	8,706.98 ± 11.33^{d}	9,610.15 ± 4.67^{c}	8,641.94 ± 25.23^{d}	7,742.58 ± 21.55^{f}	8,534.73 ± 13.49^{e}	7,580.24 ± 9.50^{g}	7,126.95 ± 9.79^{h}
Adhesiveness (g·s)	-17.85 ± 0.55^{b}	-13.72 ± 1.88^{a}	-14.30 ± 2.68^{ab}	-16.33 ± 0.66^{ab}	-13.38 ± 0.12^{a}	-12.57 ± 0.61^{a}	-13.82 ± 1.66^{ab}	-13.08 ± 0.89^{a}	-12.90 ± 1.30^{a}
Springiness (mm)	0.79 ± 0.01^{a}	0.77 ± 0.06^{a}	0.79 ± 0.00^{a}	0.80 ± 0.02^{a}	0.78 ± 0.01^{a}	0.57 ± 0.25^{a}	0.85 ± 0.02^{a}	0.80 ± 0.03^{a}	0.80 ± 0.03^{a}
Cohesiveness	0.65 ± 0.01^{a}	0.62 ± 0.03^{ab}	0.62 ± 0.01^{ab}	0.61 ± 0.01^{abc}	0.57 ± 0.01^{bc}	0.59 ± 0.01^{abc}	0.56 ± 0.01^{bc}	0.57 ± 0.02^{abc}	0.54 ± 0.00^{c}
Gumminess (g)	7,537.87 ± 5.85^{a}	5,527.89 ± 19.07^{c}	4,953.08 ± 22.31^{e}	6,582.01 ± 4.36^{b}	5,428.99 ± 13.01^{d}	4,729.85 ± 3.05^{f}	4,555.40 ± 22.72^{g}	4,026.31 ± 13.71^{h}	3,830.24 ± 10.05^{i}
Chewiness (g·mm)	5,573.13 ± 9.50^{a}	4,362.01 ± 12.21^{c}	3,339.17 ± 9.49^{c}	5,451.10 ± 9.48^{b}	4,041.05 ± 9.59^{d}	3,231.82 ± 9.98^{f}	5,440.36 ± 25.30^{b}	3,721.49 ± 2.66^{e}	3,266.81 ± 27.49^{f}
Resilience	0.49 ± 0.01^{a}	0.45 ± 0.04^{a}	0.49 ± 0.01^{a}	0.46 ± 0.01^{a}	0.45 ± 0.01^{a}	0.47 ± 0.01^{a}	0.44 ± 0.01^{a}	0.46 ± 0.03^{a}	0.44 ± 0.03^{a}

Values are expressed as means ± SEM (n = 3). Different superscript letters within a row indicate significant differences ($p < 0.05$). SPI4, SPI6, and SPI8 represent 4 %, 6 %, and 8 % soy protein isolate (SPI), respectively. SPI4C0.5, SPI6C0.5, and SPI8C0.5 denote 4 %, 6 %, and 8 % SPI with 0.5 % carrageenan, while SPI4C1, SPI6C1, and SPI8C1 indicate 4 %, 6 %, and 8 % SPI with 1 % carrageenan.

3. Results and discussion

3.1. Physicochemical properties of rice-shaped SPI–alginate–carrageenan hydrogel systems

The physicochemical properties of the rice-shaped SPI–alginate–carrageenan hydrogel are summarized in Table 1. Yield (%) increased significantly ($p < 0.05$) with increasing SPI concentration, from 63.76 ± 1.68% (SPI4) to 71.12 ± 1.87% (SPI8). The addition of carrageenan was also associated with higher yield values, with SPI8C1 showing the highest value (75.82 ± 2.83%). Although the differences between 0.5% and 1% carrageenan were not statistically significant for most SPI concentrations, formulations containing 1% carrageenan tended to show slightly higher yields. This may be associated with the contribution of carrageenan sulfate ester groups to calcium-mediated associations within the alginate-based hydrogel matrix (Alam et al., 2024; Udo et al., 2023).

Water absorption (%) also increased significantly ($p < 0.05$) with increasing SPI concentration, from 16.41 ± 2.48% (SPI4) to 26.32 ± 3.67% (SPI8). Carrageenan supplementation further enhanced hydration capacity, with SPI8C0.5 and SPI8C1 exhibiting 27.89 ± 0.23% and 29.60 ± 1.37%, respectively. These results suggest that carrageenan incorporation may contribute to increased hydration behavior within the hydrogel matrix (Lei et al., 2022).

Encapsulation efficiency (%EE) increased with both SPI concentration and carrageenan addition. The %EE increased from 50.86 ± 0.56% in SPI4 to 60.67 ± 0.22% in SPI8 and further increased to 70.86 ± 0.05% and 81.08 ± 1.53% in SPI8C0.5 and SPI8C1, respectively ($p < 0.05$). The higher %EE in carrageenan-containing formulations may be associated with additional calcium-mediated associations between carrageenan sulfate ester groups and alginate carboxylate groups, which could improve SPI retention within the hydrogel matrix. Similar trends have been reported in alginate–carrageenan systems used for bioactive compound and probiotic encapsulation (Saeed et al., 2024; Vaishnav et al., 2025). These findings indicate formulation-dependent differences in SPI retention within the hydrogel matrix.

Color parameters (L^*, a^*, b^*) were significantly influenced by SPI concentration and carrageenan incorporation ($p < 0.05$). Lightness (L^*) decreased progressively with increasing SPI content, from 41.61 ± 0.23 (SPI4) to 40.91 ± 0.07 (SPI8), and further to 39.61 ± 0.12 in SPI8C1, indicating a darker appearance at higher protein levels. Redness (a^*) increased with SPI concentration, reaching 1.07 ± 0.11 in SPI8, while carrageenan-containing formulations showed comparable values. A similar trend was observed for yellowness (b^*), with the highest value recorded in SPI8 (15.35 ± 0.15), followed by slightly lower values in SPI8C0.5 and SPI8C1. Overall, SPI concentration exerted a more pronounced effect on color development than carrageenan addition. The darker and more yellowish tones at higher SPI levels are likely attributable to the intrinsic pigmentation of soy proteins and increased solid content, which enhance light absorption and reduce reflectance (Chen et al., 2022).

3.2. Appearance

The external appearance of the rice-shaped SPI–alginate–carrageenan hydrogel samples is shown in Fig. 1. All formulations formed translucent rice-shaped particles; however, formulation-dependent surface variations were observed. Samples without carrageenan (SPI4, SPI6, SPI8) exhibited smoother surfaces with slight swelling, whereas carrageenan-containing formulations (SPI4C1, SPI6C1, SPI8C1) showed more compact and glossier surfaces. These characteristics may be associated with changes in hydrogel matrix organization due to carrageenan incorporation. Carrageenan sulfate ester groups may participate in calcium-mediated associations with alginate, potentially contributing to denser surface characteristics (Gao et al., 2024). Similar effects have been reported in carrageenan–protein co-encapsulation systems for probiotics and polyphenols, where co-polysaccharide interactions were associated with reduced surface porosity and improved particle uniformity (Dong et al., 2013). The rice-shaped morphology in the present study was evaluated as a formulation-dependent structural characteristic of the hydrogel systems. Future studies involving sensory evaluation and cooking performance assessment may further clarify the practical applicability of these rice-shaped hydrogel formulations.

3.3. Texture profile analysis

Texture profile analysis (TPA) was used to evaluate formulation-dependent textural properties influenced by SPI and carrageenan incorporation (Table 1). Hardness decreased significantly ($p < 0.05$) as SPI concentration increased, suggesting that higher protein levels may have modified the continuity and rigidity of the alginate-based gel matrix. The incorporation of carrageenan further reduced hardness, particularly at 1%, resulting in softer matrices compared with formulations containing 0.5% carrageenan. This pattern suggests that increasing carrageenan concentration may influence matrix organization and flexibility within the hydrogel system (Wang et al., 2021).

All formulations exhibited negative adhesiveness values, indicating a non-sticky texture under the test conditions. Springiness and resilience did not differ significantly among treatments ($p > 0.05$), suggesting that elasticity-related parameters were relatively maintained regardless of SPI or carrageenan content.

Gumminess and chewiness decreased with increasing SPI concentration and carrageenan addition, with the lowest values observed in formulations containing 1% carrageenan. These reductions suggest lower resistance to mastication and a softer texture profile, consistent with previous findings in soy protein–starch systems where protein–hydrocolloid interactions were associated with reduced cohesiveness and rigidity (Chen et al., 2022). The observed textural modifications may be associated with changes in the protein–polysaccharide matrix, in which carrageenan incorporation could contribute to matrix flexibility and cohesion through calcium-mediated associations. Further studies evaluating texture changes during cooking, reheating, and storage may provide additional insight into the practical performance of these hydrogel formulations (Lu et al., 2023).

3.4. Principal Component Analysis (PCA)

Principal component analysis (PCA) was used as a supportive multivariate tool to summarize the relationships among physicochemical, textural, and encapsulation parameters (Fig. 2). The first two principal components explained 87.4% of the total variance, with PC1

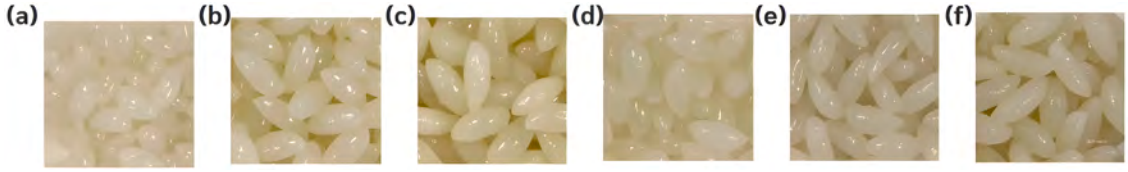

Fig. 1. Photographs of soy protein isolate (SPI) rice-shaped formulations prepared with 4 %, 6 %, and 8 % SPI (a–c: SPI4, SPI6, SPI8) in alginate (1.8 % w/v) matrices without carrageenan and with 1 % carrageenan (d–f: SPI4C1, SPI6C1, SPI8C1).

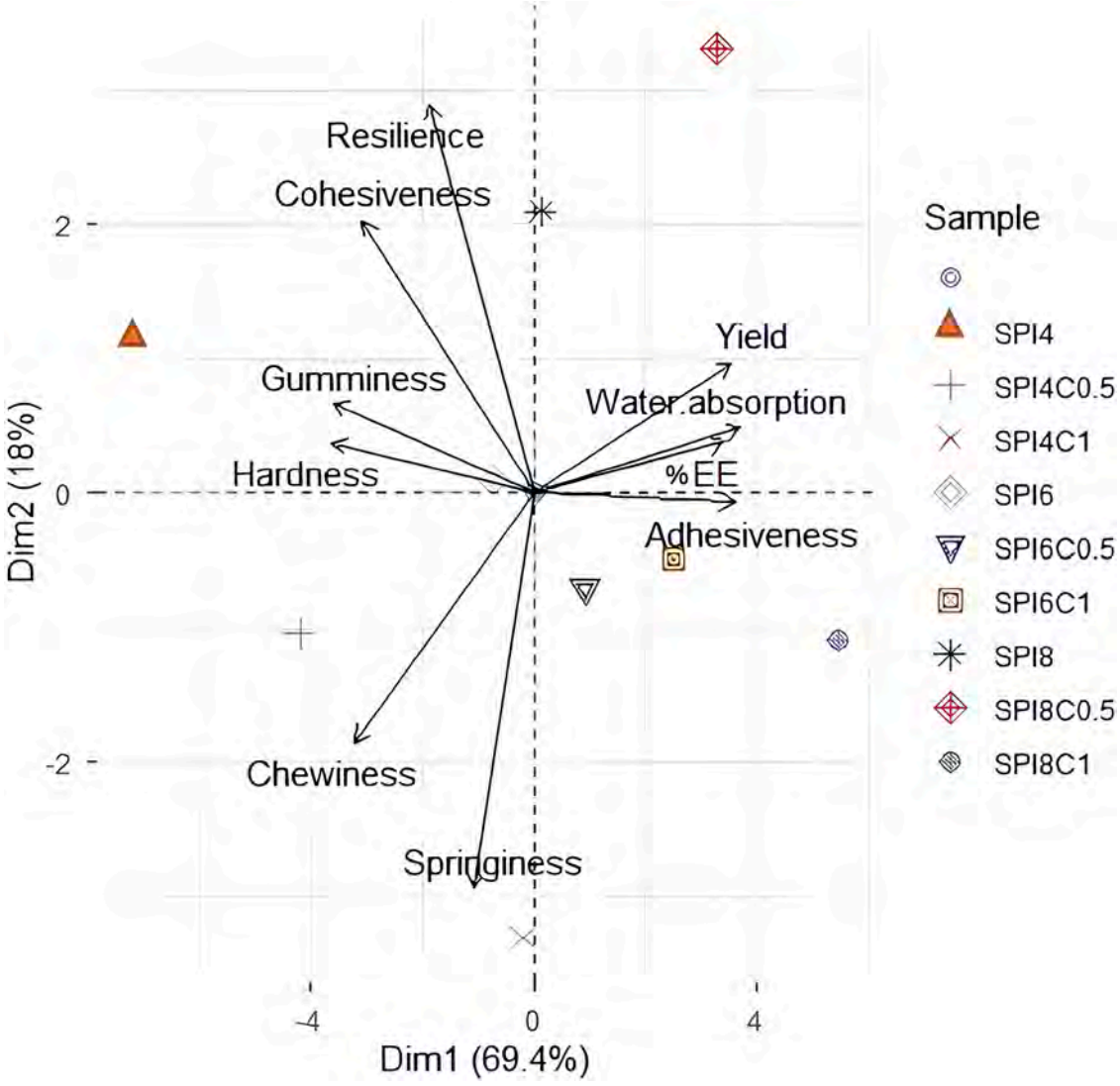

Fig. 2. Principal component analysis (PCA) correlation circle showing relationships among encapsulation efficiency, yield, water absorption, and texture parameters for SPI-based rice-shaped formulations (SPI4C0.5, SPI6C0.5, SPI8C0.5).

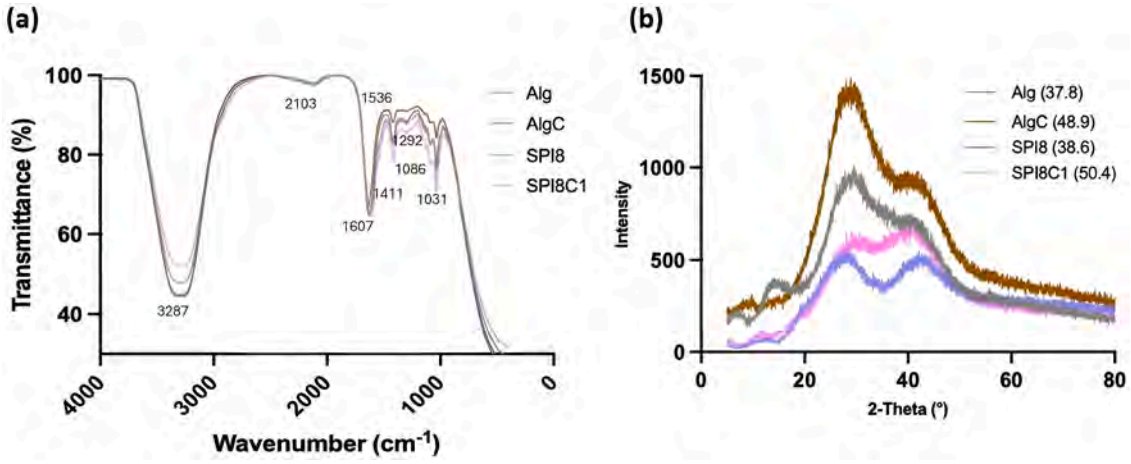

Fig. 3. Structural characterization of SPI-based rice-shaped formulations. (a) Fourier transform infrared (FTIR) spectra. (b) X-ray diffraction (XRD) patterns and relative crystallinity (%). Formulations include alginate (Alg), alginate with carrageenan (AlgC), 8 % soy protein isolate (SPI8), and 8 % soy protein isolate with 1 % carrageenan (SPI8C1).

accounting for 69.4% and PC2 accounting for 18.0% (Jolliffe and Cadima, 2016).

The PCA biplot showed formulation-dependent clustering mainly according to SPI concentration and carrageenan incorporation. Variables such as yield, water absorption, encapsulation efficiency, and adhesiveness were oriented toward the positive side of PC1, while hardness, gumminess, and chewiness were associated with the opposite direction. Formulations with higher SPI content and carrageenan addition, including SPI8C0.5 and SPI8C1, were positioned closer to variables related to hydration and encapsulation efficiency, whereas lower-SPI formulations were more closely associated with firmer textural parameters.

These clustering patterns were generally consistent with the trends observed in the physicochemical and texture results. Therefore, PCA supports the overall observation that SPI concentration and carrageenan incorporation influenced formulation-dependent properties of the hydrogel systems. However, PCA should be interpreted as a visualization and data-reduction tool rather than direct mechanistic evidence of protein–polysaccharide interactions, hydrogel network formation, or digestion-associated release behavior (Gao et al., 2024).

3.5. Fourier Transform Infrared Spectroscopy (FTIR) analysis

FTIR spectra were analyzed to examine formulation-dependent structural features of the rice-shaped SPI–alginate–carrageenan hydrogel formulations (Fig. 3a). All samples displayed characteristic absorption bands of soy protein at approximately 3280 cm^{-1} (O–H and N–H stretching), 1630–1650 cm^{-1} (amide I, C=O stretching), and 1535 cm^{-1} (amide II, N–H bending). Alginate-specific peaks were observed around 1410 cm^{-1} (asymmetric COO^- stretching) and 1030 cm^{-1} (C–O–C stretching), while carrageenan-containing formulations exhibited an additional band near 1220 cm^{-1} attributed to sulfate ester vibrations (Pasban et al., 2024). No major shifts in peak positions were detected, suggesting that the primary chemical structures of SPI, alginate, and carrageenan were largely retained during hydrogel formation. However, variations in peak intensity were evident among formulations. The amide I and II bands appeared more intense in protein-rich samples (SPI8 and SPI8C1), reflecting higher SPI content. SPI8C1 also showed greater absorption near 1220 cm^{-1}, consistent with the presence of sulfate ester groups from carrageenan in the hydrogel matrix. These intensity changes suggest possible non-covalent interactions, including hydrogen bonding, electrostatic associations, and calcium-mediated interactions among SPI, alginate, and carrageenan (Wei et al., 2025). Overall, the FTIR findings support formulation-dependent structural differences among the hydrogel systems.

3.6. X-ray Diffraction (XRD) analysis

XRD analysis was conducted to evaluate the crystalline and amorphous characteristics of the rice-shaped SPI–alginate–carrageenan hydrogel formulations (Fig. 3b). The alginate control (Alg) exhibited a broad amorphous halo, typical of alginate-based hydrogels, indicating limited molecular order. The addition of carrageenan (AlgC) was associated with increased relative crystallinity, suggesting possible changes in molecular arrangement within the alginate–carrageenan matrix (Prasetyaningrum et al., 2021).

Incorporation of SPI produced a semi-crystalline pattern, which may reflect partial ordering of soy protein chains within the alginate matrix. The presence of carrageenan further influenced this organization, with SPI8C1 displaying the highest crystallinity among the tested formulations. This increased crystallinity may be associated with closer molecular packing and greater intermolecular association within the protein–polysaccharide composite system. The observed increase in crystallinity was generally consistent with the higher encapsulation efficiency and water absorption of SPI8C1 (Table 1). The observed differences in crystallinity may be associated with formulation-dependent variations in matrix organization and hydration-related behavior under the applied experimental conditions (Lu et al., 2023). Taken together, the XRD and FTIR findings suggest differences in structural organization among the tested formulations. Further rheological and microstructural characterization may provide additional insight into the structural properties of these hydrogel systems.

3.7. Digestion-associated release of amino-group-containing residues and selected phytochemical compounds

Fig. 4 presents the release-associated profiles of amino-group-containing residues, Folin–Ciocalteu-reactive phenolic-associated compounds, selected isoflavone-associated compounds, and antioxidant-related responses from SPI–alginate–carrageenan hydrogel formulations during simulated gastrointestinal digestion.

The release of amino-group-containing residues (Fig. 4a), assessed using the ninhydrin assay, differed significantly among formulations ($p < 0.05$). SPI-containing samples, particularly SPI8 and SPI8C1, showed higher ninhydrin responses than alginate controls. The ninhydrin assay detects free amino groups derived from amino acids, peptides, and other amino-group-containing compounds in the digestion medium. Therefore, the observed responses were interpreted as digestion-associated release behavior under the applied in vitro conditions.

SPI8C1 exhibited the highest overall ninhydrin response, which may partly reflect its higher initial SPI concentration in the formulation. Carrageenan-containing matrices may have contributed to SPI retention

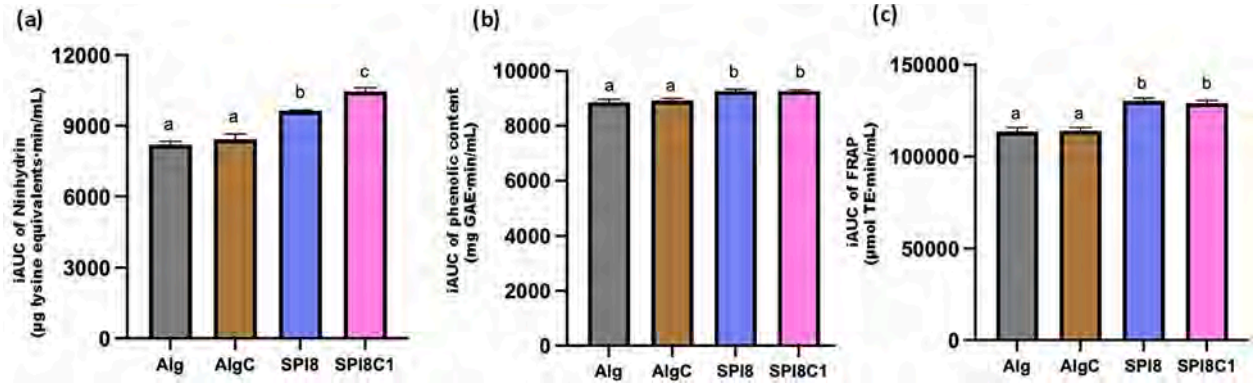

Fig. 4. Digestion-associated release profiles of rice-shaped SPI–alginate–carrageenan hydrogel formulations. Incremental area under the curve (iAUC) values of (a) release of amino-group-containing residues determined by the ninhydrin assay, (b) Folin–Ciocalteu-reactive phenolic-associated compounds, and (c) antioxidant-related responses determined by the FRAP assay under simulated gastrointestinal digestion conditions. Formulations include alginate (Alg), alginate with carrageenan (AlgC), 8% soy protein isolate (SPI8), and 8% soy protein isolate with 1% carrageenan (SPI8C1).

Table 2
Isoflavone content (μg/g sample) in soy protein isolate (SPI)–based rice-shaped formulations before digestion.

Samples	Isoflavone compounds (μg/g sample)		
	Genistin	Daidzin	Genistein
Alg	nd	nd	nd
AlgC	nd	nd	nd
SPI8	2.97 ± 0.06[a]	1.09 ± 0.05[a]	2.01 ± 0.08[a]
SPI8C1	2.77 ± 0.04[a]	0.91 ± 0.01[b]	1.76 ± 0.10[a]

Values are expressed as means ± SEM (n = 3). Different superscript letters within a column indicate significant differences ($p < 0.05$). All samples are rice-shaped formulations prepared with alginate-based matrices. Alg represents alginate; AlgC represents alginate with carrageenan; SPI8 indicates 8 % soy protein isolate; SPI8C1 indicates 8 % soy protein isolate with 1 % carrageenan; nd = not detected.

Table 3
Isoflavone release (μg/mL) in digesta from soy protein isolate (SPI)–based rice-shaped formulations after simulated gastrointestinal digestion.

Samples	Isoflavone compounds (μg/mL)		
	Genistin	Daidzin	Genistein
Alg	nd	nd	nd
AlgC	nd	nd	nd
SPI8	0.23 ± 0.02[a]	nd	nd
SPI8C1	0.28 ± 0.03[a]	nd	nd

Values are expressed as means ± SEM (n = 3). Different superscript letters within a column indicate significant differences ($p < 0.05$). All samples are soy protein isolate (SPI)–based rice-shaped formulations prepared with alginate matrices. Alg represents alginate; AlgC represents alginate with carrageenan; SPI8 indicates 8 % soy protein isolate; SPI8C1 indicates 8 % soy protein isolate with 1 % carrageenan; nd = not detected.

during preparation and subsequent digestion-associated release under the present *in vitro* conditions, but this should not be considered evidence of controlled release or enhanced digestibility (Mahdavinia et al., 2014).

Folin–Ciocalteu-reactive phenolic-associated compounds (Fig. 4b) also varied significantly among formulations. SPI8 and SPI8C1 showed higher values than alginate-only controls ($p < 0.05$). These differences may be associated with the release of reducing compounds during simulated digestion, including phenolic-associated compounds and other Folin–Ciocalteu-reactive substances. Enzymatic disruption of matrix components and pH-dependent solubility changes may contribute to these responses (Ribas-Agustí et al., 2018).

Isoflavone profiles (Tables 2 and 3) showed low but detectable levels of selected isoflavone-associated compounds in SPI-containing formulations. In the present study, genistin, daidzin, and genistein were selected as targeted analytes because authentic standards were available for compound confirmation and external calibration. Non-digested SPI8 and SPI8C1 contained detectable isoflavone-associated compounds, while low but detectable genistin levels were observed after digestion. The relatively low levels of released isoflavone-associated compounds may be associated with the limited native isoflavone content of the SPI used in the formulation and possible interactions between isoflavones and the protein–polysaccharide hydrogel matrix under the applied digestion conditions. These findings indicate formulation-dependent differences in selected isoflavone-associated compounds under the applied in vitro conditions. Similar observations have been reported in alginate–carrageenan systems associated with compound retention and release behavior during simulated digestion (Tang et al., 2025).

Antioxidant-related responses (Fig. 4c), evaluated by the FRAP assay, showed formulation-dependent differences that generally followed the trends observed for phenolic-associated compounds. SPI-containing formulations exhibited higher FRAP values than alginate controls ($p < 0.05$). Although SPI8C1 showed marginally lower FRAP values than SPI8, the difference was not significant. These findings suggest that formulation composition influenced antioxidant-related chemical responses under the applied in vitro conditions.

Overall, the digestion-associated release results indicate that SPI concentration and carrageenan incorporation influenced release-associated responses under the simplified simulated gastrointestinal conditions used in this study. The observed formulation-dependent differences may be associated with variations in matrix organization, SPI retention, and hydration behavior among the hydrogel systems. Further studies using standardized digestion models and comparative analyses with free SPI may provide additional insight into formulation-dependent release behavior.

4. Conclusion

This study provides proof-of-concept information on the formulation-dependent physicochemical, structural, and digestion-associated release properties of rice-shaped SPI–alginate–carrageenan hydrogel systems. Increasing SPI concentration and carrageenan incorporation influenced product yield, water absorption, encapsulation efficiency, texture, morphology, and matrix organization. Among the tested formulations, SPI8C1 exhibited the highest encapsulation efficiency and the greatest amino-group-containing equivalent response measured by the ninhydrin assay, while carrageenan-containing formulations showed differences in hydration behavior and structural organization compared with alginate-only systems. FTIR and XRD analyses further supported formulation-dependent differences in molecular organization and crystallinity among the hydrogel formulations. In addition, targeted LC–MS analysis detected selected isoflavone-associated compounds, including genistin, daidzin, and genistein, in SPI-containing hydrogel systems. Overall, the findings provide preliminary insight into the development of rice-shaped plant protein hydrogel formulations using SPI, alginate, and carrageenan as structuring components. Further studies using standardized digestion models, sensory evaluation, and practical processing assessments are warranted to clarify the broader applicability of these hydrogel systems in food applications.

Ethical statement

This study did not involve any experiments with human participants or animals. All analyses were conducted using in vitro methods, and therefore ethical approval was not required.

CRediT authorship contribution statement

Mutthatinee Tangmongkhonsuk: Writing – review & editing, Writing – original draft, Visualization, Validation, Project administration, Methodology, Investigation, Formal analysis, Data curation, Conceptualization. **Siriyakorn Chantieng:** Data curation. **Vernabelle Balmori:** Software, Data curation. **Kasinee Katelakha:** Data curation. **Nureesun Mahamud:** Data curation. **Charoonsri Chusak:** Investigation. **Nazimah Hamid:** Writing – review & editing, Data curation. **Sirichai Adisakwattana:** Writing – review & editing, Visualization, Supervision, Resources, Methodology, Funding acquisition, Conceptualization.

Declaration of competing interest

The authors declare that they have no known competing financial interests or personal relationships that could have appeared to influence the work reported in this paper.

Acknowledgements

This research was financially supported by the National Research

Council of Thailand (NRCT) under grant numbers N41A661129 and N42A680622, the Second Century Fund (C2F), Chulalongkorn University, and the Ratchadapisek Somphot Fund, Chulalongkorn University (GCUGR1125682004D).

Supplementary materials

Supplementary material associated with this article can be found, in the online version, at doi:10.1016/j.fufo.2026.101109.

Data availability

Data will be made available on request.

References

AACC. (1988). Approved methods of the AACC—method 74–09.

Alam, M., Pant, K., Brar, D.S., Dar, B.N., Nanda, V., 2024. Exploring the versatility of diverse hydrocolloids to transform techno-functional, rheological, and nutritional attributes of food fillings. Food Hydrocoll. 146, 109275. https://doi.org/10.1016/j.foodhyd.2023.109275.

AOAC International, 2023. *Official methods of analysis* (Method 984.27). AOAC International.

Barańska, A., Błaszczuk, A., Polz-Dacewicz, M., Kanadys, W., Malm, M., Janiszewska, M., Jędrych, M., 2021. Effects of soy isoflavones on glycemic control and lipid profile in patients with type 2 diabetes: a systematic review and meta-analysis of randomized controlled trials. Nutrients 13 (6), 1886. https://doi.org/10.3390/nu13061886.

Chantieng, S., Balmori, V., Katelakha, K., Suantawee, T., Ngamukote, S., Chusak, C., Adisakwattana, S., 2025. Upcycling defatted rice bran into alginate based noodles via hydrocolloid assisted development and assessment of structural and functional properties. Curr. Res. Food Sci. 11, 101178. https://doi.org/10.1016/j.crfs.2025.101178.

Chaturvedi, S., Manickavasagan, A., 2024. Rice analogues: processing methods and product quality. Trends Food Sci. Technol. 148, 104493. https://doi.org/10.1016/j.tifs.2024.104493.

Chen, Q., Zhang, J., Zhang, Y., Kaplan, D.L., Wang, Q., 2022. Protein-amylose/amylopectin molecular interactions during high-moisture extruded texturization toward plant-based meat substitutes applications. Food Hydrocoll. 127, 107559. https://doi.org/10.1016/j.foodhyd.2022.107559.

Chusak, C., Chanbunyawat, P., Chumnumduang, P., Chantarasinlapin, P., Suantawee, T., Adisakwattana, S., 2020. Effect of gac fruit (*Momordica cochinchinensis*) powder on in vitro starch digestibility, nutritional quality, textural and sensory characteristics of pasta. LWT 118, 108856. https://doi.org/10.1016/j.lwt.2019.108856.

Dong, Q.-Y., Chen, M.-Y., Xin, Y., Qin, X.-Y., Cheng, Z., Shi, L.-E., Tang, Z.-X., 2013. Alginate-based and protein-based materials for probiotics encapsulation: a review. Int. J. Food Sci. Technol. 48 (7), 1339–1351. https://doi.org/10.1111/ijfs.12078.

EFSA ANS Panel (EFSA Panel on Food Additives and Nutrient Sources added to Food), 2012. Guidance for submission for food additive evaluations. EFSA Journal 10(7), 2760. https://doi.org/10.2903/j.efsa.2012.2760.

Gao, Y., Liu, R., Liang, H., 2024. Food hydrocolloids: structure, properties, and applications. Foods 13 (7), 1077. https://doi.org/10.3390/foods13071077.

Hertzler, S.R., Lieblein-Boff, J.C., Weiler, M., Allgeier, C., 2020. Plant proteins: assessing their nutritional quality and effects on health and physical function. Nutrients 12 (12), 3704. https://doi.org/10.3390/nu12123704.

Huang, Y., Liu, L., Sun, B., Zhu, Y., Lv, M., Li, Y., Zhu, X., 2024. A comprehensive review on harnessing soy proteins in the manufacture of healthy foods through extrusion. Foods 13 (14), 2215. https://doi.org/10.3390/foods13142215.

Jolliffe, I.T., Cadima, J., 2016. Principal component analysis: a review and recent developments. Philos. Trans. R. Soc. A 374 (2065), 20150202. https://doi.org/10.1098/rsta.2015.0202.

Lai, H., Sun, M., Liu, Y., Zhu, H., Li, M., Pan, B., Wang, Q., Yang, Q., Cao, X., Tian, C., 2023. White rice consumption and risk of cardiometabolic and cancer outcomes: a systematic review and dose-response meta-analysis of prospective cohort studies. Crit. Rev. Food Sci. Nutr. 63 (33), 12476–12487. https://doi.org/10.1080/10408398.2022.2101984.

Lee, K.Y., Mooney, D.J., 2012. Alginate: properties and biomedical applications progress in polymer. science 37 (1), 106–126. https://doi.org/10.1016/j.progpolymsci.2011.06.003.

Lei, Y.C., Zhao, X., Li, D., Wang, L.J., Wang, Y., 2022. Effects of κ-carrageenan and guar gum on the rheological properties and microstructure of phycocyanin gel. Foods 11 (5), 734. https://doi.org/10.3390/foods11050734.

Lu, Z., Lee, P.-R., Yang, H., 2023. Kappa-carrageenan improves the gelation and structures of soy protein isolate through the formation of hydrogen bonding and electrostatic interactions. Food Hydrocoll. 140, 108585. https://doi.org/10.1016/j.foodhyd.2023.108585.

Mahdavinia, G.R., Rahmani, Z., Karami, S., Pourjavadi, A., 2014. Magnetic/pH-sensitive κ-carrageenan/sodium alginate hydrogel nanocomposite beads: preparation, swelling behavior, and drug delivery. J. Biomater. Sci. 25 (17), 1891–1906. https://doi.org/10.1080/09205063.2014.956166. Polymer Edition.

National Academies of Sciences, Engineering, and Medicine, 2011. Dietary reference intakes for calcium and vitamin D. National Academies Press. https://doi.org/10.17226/13050.

Pasban, A., Mousavi, S.F., Abdollahi, S., Hesarinejad, M.A., 2024. Evaluating the potential of soy protein isolate/alginate hydrogel as polyphenolic liposome carrier during gastrointestinal tract: a case study on sumac extract. LWT 211, 116883. https://doi.org/10.1016/j.lwt.2024.116883.

Peanparkdee, M., Patrawart, J., Iwamoto, S., 2019. Effect of extraction conditions on phenolic content, anthocyanin content and antioxidant activity of bran extracts from Thai rice cultivars. J. Cereal. Sci. 86, 86–91. https://doi.org/10.1016/j.jcs.2019.01.011.

Postolović, K.S., Antonijević, M.D., Ljujić, B., Miletić Kovačević, M., Gazdić Janković, M., Stanić, Z.D., 2022. pH-responsive hydrogel beads based on alginate, κ-carrageenan and poloxamer for enhanced curcumin, natural bioactive compound, encapsulation and controlled release efficiency. Molecules 27 (13), 4045. https://doi.org/10.3390/molecules27134045.

Prasetyaningrum, A., Utomo, D.P., Raemas, A.F.A., Kusworo, T.D., Jos, B., Djaeni, M., 2021. Alginate/κ-carrageenan-based edible films incorporated with clove essential oil: physico-chemical characterization and antioxidant-antimicrobial activity. Polymers. (Basel) 13 (3), 354. https://doi.org/10.3390/polym13030354.

R Core Team, R, 2020. R: A language and environment for statistical computing. Citeseer.

Ren, C., Xiong, W., Peng, D., He, Y., Zhou, P., Li, J., Li, B., 2018. Effects of thermal sterilization on soy protein isolate/polyphenol complexes: aspects of structure, in vitro digestibility and antioxidant activity. Food Res. Int. 112, 284–290. https://doi.org/10.1016/j.foodres.2018.06.034.

Ribas-Agustí, A., Martín-Belloso, O., Soliva-Fortuny, R., Elez-Martínez, P., 2018. Food processing strategies to enhance phenolic compounds bioaccessibility and bioavailability in plant-based foods. Crit. Rev. Food Sci. Nutr. 58 (15), 2531–2548. https://doi.org/10.1080/10408398.2017.1331200.

Saeed, M., Khanam, R., Hafeez, H., Ahmad, Z., Saleem, S., Tariq, M.R., Safdar, W., Waseem, M., Ali, U., Azam, M., 2024. Viability of free and alginate–carrageenan gum coated *Lactobacillus acidophilus* and *Lacticaseibacillus casei* in functional cottage cheese. ACS Omega 9 (12), 13840–13851. https://doi.org/10.1021/acsomega.3c08588.

Suklaew, P.O., Chusak, C., Adisakwattana, S., 2020. Physicochemical and functional characteristics of RD43 rice flour and its food application. Foods 9 (12), 1912. https://doi.org/10.3390/foods9121912.

Tang, Y., Liu, W., Zhang, J., Juan, B., Zhu, Y., Zhu, L., Zhao, Y., Daglia, M., Xiao, X., He, Y., 2025. Advances in intestinal-targeted release of phenolic compounds. Nutrients 17 (16), 2598. https://doi.org/10.3390/nu17162598.

Udo, T., Mummaleti, G., Mohan, A., Singh, R.K., Kong, F., 2023. Current and emerging applications of carrageenan in the food industry. Food Res. Int. 173, 113369. https://doi.org/10.1016/j.foodres.2023.113369.

Vaishnav, A., Mehta, N.K., Priyadarshini, M.B., Singh, S.K., Acharya, P.C., Biswal, S., Nath, H., Hussain, S.A., Pal, P., Lal, J., 2025. Impact of carrageenan-based encapsulation on the physicochemical, structural, and antioxidant properties of freshwater snail (*Bellamya bengalensis*) protein hydrolysates. Colloids Interfaces 9 (3), 29. https://doi.org/10.3390/colloids9030029.

Vatansever, S., Chen, B., Hall, C., 2024. Plant protein flavor chemistry fundamentals and techniques to mitigate undesirable flavors. Sustainable Food Proteins 2 (1), 33–57. https://doi.org/10.1002/sfp2.1025.

Wang, X., Zhou, D., Guo, Q., Liu, C., 2021. Textural and structural properties of a κ-carrageenan–konjac gum mixed gel: effects of κ-carrageenan concentration, mixing ratio, sucrose and Ca2+ concentrations and its application in milk pudding. J. Sci. Food Agric. 101 (7), 3021–3029. https://doi.org/10.1002/jsfa.10936.

Wei, Y., Lin, S., Lin, W., Nie, Y., Zou, X., Zheng, Y., Li, B., He, Y., Huang, Y., Huang, Y., 2025. The impact of κ-Carrageenan on the textural, microstructural, and molecular properties of heat-induced egg white protein gel. Food Sci. Nutr. 13 (8), e70541. https://doi.org/10.1002/fsn3.70541.

Wongverawattanakul, C., Suklaew, P.O., Chusak, C., Adisakwattana, S., Thilavech, T., 2022. Encapsulation of *Mesona chinensis* benth extract in alginate beads enhances the stability and antioxidant activity of polyphenols under simulated gastrointestinal digestion. Foods 11 (15), 2378. https://doi.org/10.3390/foods11152378.

Xie, L., Lu, L., Zhao, L., Peng, J., Zhou, W., 2025. Improvement of okara noodle quality by modifying the soluble/insoluble dietary fibre ratio. Food Chem. 464, 141566. https://doi.org/10.1016/j.foodchem.2024.141566.